ELSEVIER

Surface Science 454–456 (2000) 918–924

surface science

www.elsevier.nl/locate/susc

The CPP transport in metallic magnetic multilayers

J. Kudrnovský [a,*], V. Drchal [a], I. Turek [b], C. Blaas [c], P. Weinberger [c], P. Bruno [d]

[a] *Institute of Physics, Academy of Sciences of the Czech Republic, Na Slovance 2, CZ-182 21 Prague 8, Czech Republic*
[b] *Institute of Physics of Materials, Academy of Sciences of the Czech Republic, Žižkova 22, CZ-616 62 Brno, Czech Republic*
[c] *Center for Computational Materials Science and Institute for Technical Electrochemistry and Solid State Chemistry, Technical University of Vienna, Getreidemarkt 9/158, A-1060 Vienna, Austria*
[d] *Max-Planck Institute for Microstructure Physics, Weinberg 2, D-06120 Halle, Germany*

Abstract

The transmission matrix approach is used to evaluate perpendicular magnetotransport in metallic multilayers that consist of two magnetic slabs separated by a non-magnetic spacer. We employ the spin-polarized surface Green function technique within the framework of the tight-binding linear muffin-tin orbital method. Our approach allows both the ballistic and the diffusive regime of magnetotransport to be treated on equal footing. The effect of disorder is included in terms of lateral supercells confined to individual atomic layers. In this paper, we apply the method to fcc-based Co/Cu/Co(001) trilayers. © 2000 Elsevier Science B.V. All rights reserved.

Keywords: Cobalt; Copper; Magnetic films; Metallic films

1. Introduction

Transport in layered materials has been the subject of intensive theoretical investigations, in particular in view of the discovery of the giant magnetoconductance (GMC) in metallic multilayers [1]. Most of the measurements to date have been reported for the current-in-plane (CIP) geometry [2] since the current-perpendicular-to-plane (CPP) geometry [3] is experimentally more challenging. The CPP transport is also closely related to the tunneling through a non-metallic spacer and to the ballistic transport [4].

Ab initio calculations of the GMC are still rather rare. We mention the method of solving the Boltzmann equation applied to multilayers [5] and a Kubo–Greenwood approach generalized to layered systems in terms of the Layer Korringa–Kohn–Rostoker (KKR) method [6] as well as in terms of the relativistic spin-polarized screened KKR method [7,8] but neglecting vertex corrections with respect to the configurational average of the products of two single-particle Green functions. Both approaches can, at least in principle, be used for CIP as well as for CPP.

Alternative theoretical approaches applicable to the CPP transport are based either on a non-equilibrium Green function method [9] or on a transmission matrix formalism [10–12] and were implemented within an empirical tight-binding (TB) method based on surface Green functions (SGFs).

In this paper, we will formulate such an approach within the first-principles tight-binding linear muffin-tin orbital (TB-LMTO) method [13] for a general stacking of non-random layers (ballistic transport). This formulation will then be

* Corresponding author. Fax: +420-2-858-8605.
E-mail address: kudrnov@fzu.cz (J. Kudrnovský)

PII: S0039-6028(00)00069-8

extended to the case of lateral two-dimensional supercells within each disordered atomic layer. The usefulness of such an approach has recently been illustrated for the case of a single-band TB model [14].

2. Formalism

Suppose the magnetic multilayer system consists of a semi-infinite left (>) and a semi-infinite right (+) magnetic lead sandwiching a non-magnetic spacer of varying thickness such that, in principle, atomic layers can be viewed in terms of $n\times n$ supercells ($n\times n$ two-dimensional complex lattice). In order to describe disorder (substitutional binary alloys), it is then necessary to average over different sizes, n, of supercells and for each n over different occupations of the sites within the supercell with the two constituents involved. Clearly, such an approach applies to disordered spacers and/or to disordered interfaces. We neglect possible layer and lattice relaxations in the system: all our calculations refer to a fcc Co parent lattice.

2.1. Electronic structure

The electronic structure of the system is described by the following TB-LMTO Hamiltonian,

$$H^{\gamma;\sigma}_{\boldsymbol{RL},\boldsymbol{R}'L'} = C^{\sigma}_{\boldsymbol{RL}}\delta_{\boldsymbol{R},\boldsymbol{R}'}\delta_{L,L'} + (\Delta^{\sigma}_{\boldsymbol{RL}})^{1/2}\{S^{\beta}(1-(\gamma^{\sigma}-\beta)S^{\beta})^{-1}\}_{\boldsymbol{RL},\boldsymbol{R}'L'}(\Delta^{\sigma}_{\boldsymbol{R}'L'})^{1/2}, \tag{1}$$

where $\boldsymbol{R}$ is the site index, σ is the spin index, and the potential parameters $C^{\sigma}_{\boldsymbol{RL}}$, $\Delta^{\sigma}_{\boldsymbol{RL}}$, and $\gamma^{\sigma}_{\boldsymbol{RL}}$ are diagonal matrices with respect to the angular momentum index $L=(\ell m)$. The non-random screened structure constants matrix $S^{\beta}_{\boldsymbol{RL},\boldsymbol{R}'L'}$ and the screening matrix $\beta_{\boldsymbol{R},LL'}=\beta_L$, $\delta_{L,L'}$ are spin-independent. Assuming one and the same two-dimensional translational symmetry in each layer p, $\boldsymbol{k}_{\parallel}$-projections can be defined where $\boldsymbol{k}_{\parallel}$ is a vector from the corresponding surface Brillouin zone (SBZ). In a principal layer formalism [15], the screened structure constants, $S^{\beta}_{p,q}$, are of a block tridiagonal form. Neglecting layer relaxations, they are given by

$$S^{\beta}_{p,p}(\boldsymbol{k}_{\parallel}) = S^{\beta}_{0,0}(\boldsymbol{k}_{\parallel}),\ S^{\beta}_{p,q}(\boldsymbol{k}_{\parallel}) = S^{\beta}_{0,1}(\boldsymbol{k}_{\parallel})\delta_{p+1,q} + S^{\beta}_{1,0}(\boldsymbol{k}_{\parallel})\delta_{p-1,q}. \tag{2}$$

The properties of the individual atoms are characterized by potential function matrices,

$$P^{\beta,\sigma}_{\boldsymbol{R}}(z) = \frac{z-C^{\sigma}_{\boldsymbol{R}}}{\Delta^{\sigma}_{\boldsymbol{R}}+(\gamma^{\sigma}_{\boldsymbol{R}}-\beta)(z-C^{\sigma}_{\boldsymbol{R}})}, \tag{3}$$

which are diagonal with respect to L and are obtained by solving the corresponding Schrödinger equation within the density functional formalism. In the case of a binary substitutional alloy, the potential functions assume two different values (we thus neglect possible local environment effects within a supercell). Finally, we define the Green function matrix $g^{\beta,s}(z)$ in the TB-LMTO method as

$$(g^{\beta,\sigma}(\boldsymbol{k}_{\parallel},z))^{-1}_{p,q} = P^{\beta,\sigma}_{p}(z)\delta_{p,q} - S^{\beta}_{p,q}(\boldsymbol{k}_{\parallel}). \tag{4}$$

We refer the reader to a recent book [15] for further details concerning the TB-LMTO method for layered systems.

2.2. Magnetoconductance

Our derivation of the magnetoconductance $\mathscr{C}_M$ follows that given in Ref. [9]; its details will be published elsewhere. The subscript $M=\mathrm{F}$ (AF) denotes a ferromagnetic (antiferromagnetic) configuration of the magnetizations in the leads, respectively.

The resulting expression is given by

$$\mathscr{C}_M = \sum_{\sigma}\mathscr{C}^{\sigma}_M, \quad \mathscr{C}^{\sigma}_M = \frac{e^2}{h}\frac{1}{N_{\parallel}}\sum_{\boldsymbol{k}_{\parallel}} T^{\sigma}_M(\boldsymbol{k}_{\parallel}, E_{\mathrm{F}}), \tag{5}$$

where $N_{\parallel}$ is the number of $\boldsymbol{k}_{\parallel}$-points in the SBZ, and E_{F} is the Fermi energy. Suppressing the subscript, M, the transmission coefficient, $T^{\sigma}(\boldsymbol{k}_{\parallel}, E)$, is expressed as

$$T^{\sigma}(\boldsymbol{k}_{\parallel}, E) = \lim_{|\delta|\to 0}\ \mathrm{tr}\{B^{\beta,\sigma}_1(\boldsymbol{k}_{\parallel}, E)g^{\beta,\sigma}_{1,N}(\boldsymbol{k}_{\parallel}, z_+) \times B^{\beta,\sigma}_N(\boldsymbol{k}_{\parallel},E)g^{\beta,\sigma}_{N,1}(\boldsymbol{k}_{\parallel}, z_-)\}, \tag{6}$$

where tr denotes the trace over angular momenta,

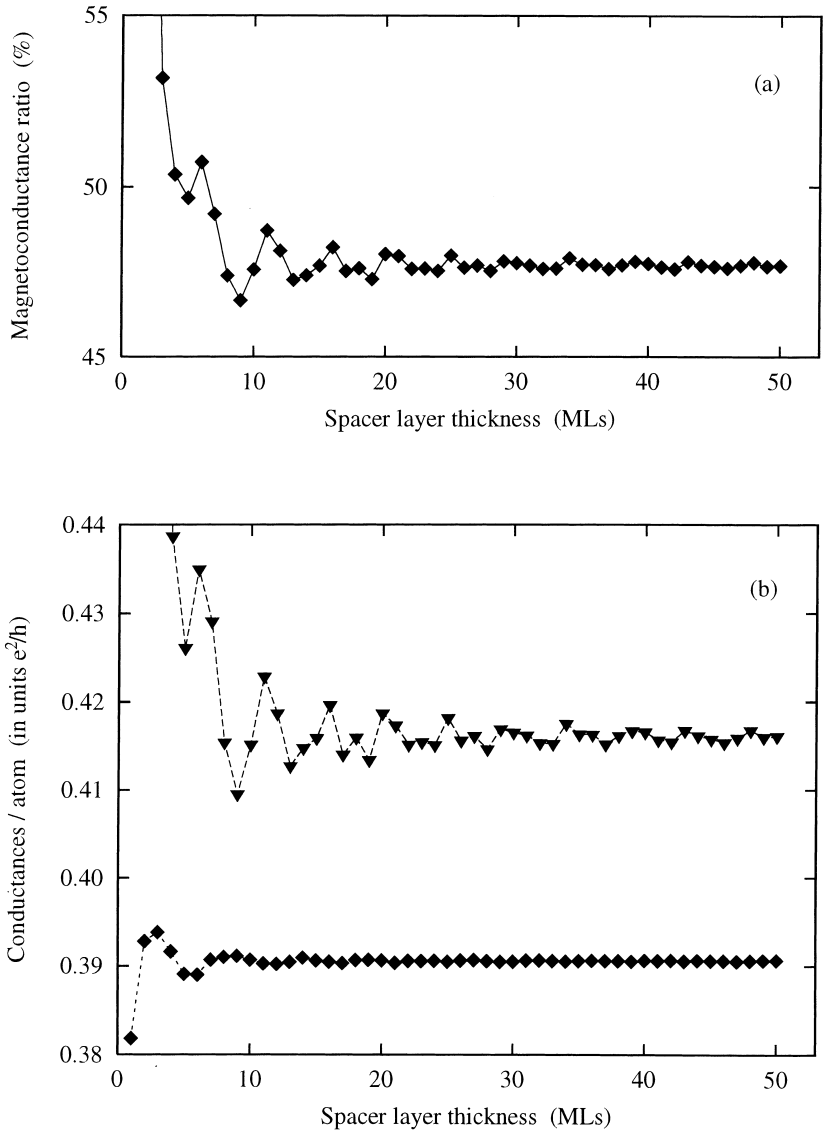

Fig. 1. Ideal Co/Cu/Co trilayer: (a) magnetoconductance ratio and (b) conductances per atom for the ferromagnetic configuration ↓-spin (inverted triangles) and for the antiferromagnetic configuration (diamonds, the same for ↑- and ↓-spins). Since the ferromagnetic ↑-spin conductances are independent of the spacer thickness, they are not shown.

L,

$$B_1^{\beta,\sigma}(E) = iS_{1,0}^{\beta}(\boldsymbol{k}_\parallel)[\mathcal{G}_{\mathcal{L}}^{\beta,\sigma}(\boldsymbol{k}_\parallel, z_+) - \mathcal{G}_{\mathcal{L}}^{\beta,\sigma}(\boldsymbol{k}_\parallel, z_-)]S_{0,1}^{\beta}(\boldsymbol{k}_\parallel),$$

$$B_N^{\beta,\sigma}(E) = iS_{0,1}^{\beta}(\boldsymbol{k}_\parallel)[\mathcal{G}_{\mathcal{R}}^{\beta,\sigma}(\boldsymbol{k}_\parallel, z_+) - \mathcal{G}_{\mathcal{R}}^{\beta,\sigma}(\boldsymbol{k}_\parallel, z_-)]S_{1,0}^{\beta}(\boldsymbol{k}_\parallel), \quad (7)$$

and $z_\pm = E \pm i\delta$. The quantities $\mathcal{G}_{\mathcal{X}}^{\beta,\sigma}$, $\mathcal{X} = \mathcal{L}$, $\mathcal{R}$, are the SGFs of the ideal left and right leads [15], respectively. The magnetoconductance ratio is then defined as $R_{\mathrm{GMC}} = \mathcal{C}_F/\mathcal{C}_{AF} - 1$.

A generalization to the case of $n \times n$ lateral supercells is straightforward: the equations remain formally identical, only the matrices are replaced

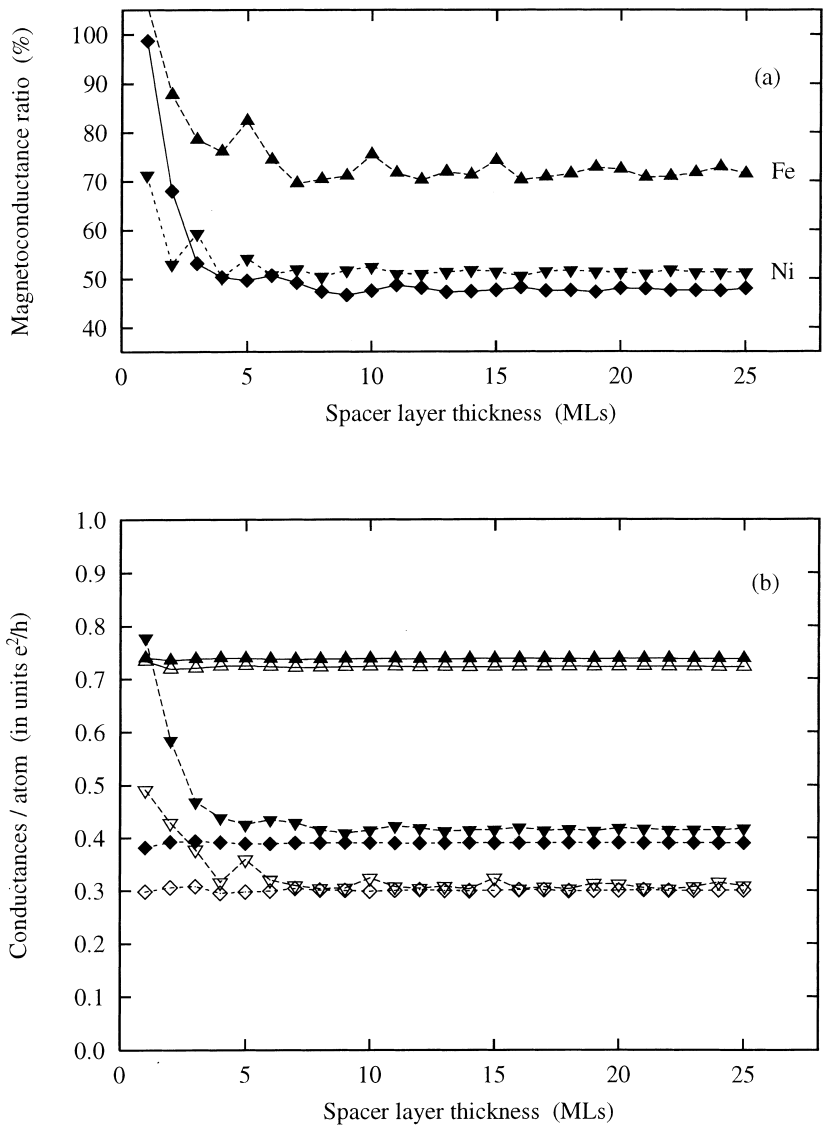

Fig. 2. $Co/X_1/Cu/X_1/Co$, X = Fe (Ni), namely trilayers with inserted Fe (Ni) monolayers at the interfaces: (a) magnetoconductance ratio for the ideal trilayer (diamonds), for the inserted Fe monolayers (triangles), and for the inserted Ni monolayers (inverted triangles) and (b) conductances per atom for the ferromagnetic configuration(↑-spin, triangles, and ↓-spin, inverted triangles) and for the antiferromagnetic configuration (diamonds, the same for ↑- and ↓-spins). The full symbols refer to the ideal trilayer, and empty symbols refer to those with inserted Fe monolayers.

by supermatrices with respect to inequivalent atoms in the supercell, and the $\boldsymbol{k}_{\parallel}$-integration is confined to the (n^2-times smaller) SBZ corresponding to the supercell.

3. Results and discussion

We performed calculations for three different systems, all with an fcc(001) stacking of layers:

(1) an ideal Co/Cu/Co trilayer (Fig. 1), (2) $Co/X_1/Cu/X_1/Co$, X = Fe (Ni), namely trilayers with inserted Fe (Ni) monolayers at the interfaces (Fig. 2), and (3) a random $Cu_{84}Ni_{16}$ spacer sandwiched by pure Co (Fig. 3). The first two cases correspond to the so-called ballistic transport, while in the last one, diffusive transport is also important. Extensive single-band TB calculations as well as realistic calculations based on the TB-LMTO method suggest that 5×5-supercells (21 A-atoms and four B-atoms) averaged over five different configurations yield representative results. The input potential functions were determined self-consistently for a given alloy composition using

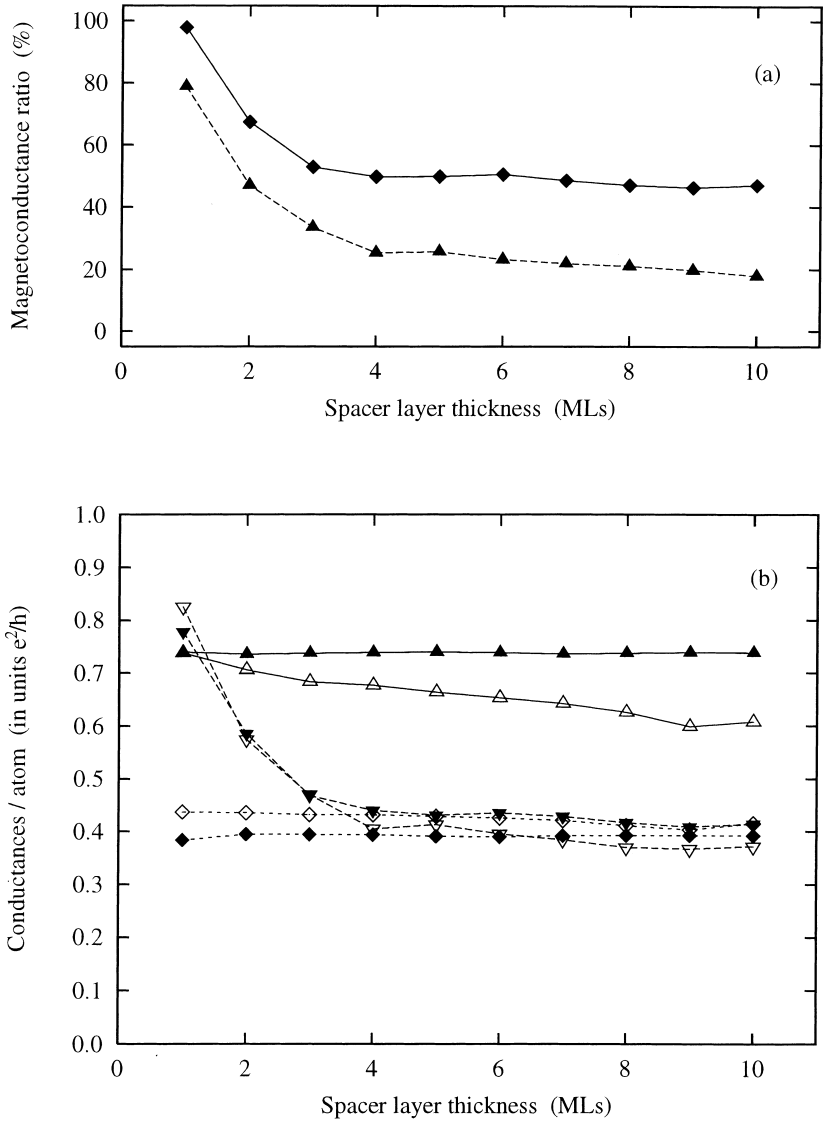

Fig. 3. $Co/Cu_{84}Ni_{16}/Co$ trilayer: (a) magnetoconductance ratio for the ideal trilayer (diamonds) and for the random spacer (triangles); (b) conductances per atom for the ferromagnetic configuration (↑-spin, triangles, and ↓-spin, inverted triangles) and for the antiferromagnetic configuration (diamonds, the same for ↑- and ↓-spins). The full symbols refer to the ideal trilayer, and empty symbols refer to the random spacer.

the coherent potential approximation (CPA) [15]. The $\boldsymbol{k}_{\parallel}$-integration extends over 10 000 points in the full fcc(001)-SBZ (400 points in the corresponding SBZ of the supercell) and $|\mathrm{Im}\, z_{\pm}| = 10^{-7}$ Ry. The GMC ratios are plotted in Figs. 1a, 2a, and 3a, whereas the F and AF conductances for ↑- and ↓-spin electrons are plotted in Figs. 1b, 2b, and 3b as a function of the spacer thickness. It should be noted that for a symmetric arrangement of atomic layers, as used here, the AF-↑ and AF-↓ conductances are identical.

3.1. Ballistic transport

The most remarkable feature found for an ideal trilayer (Fig. 1) is a strong decrease in GMC ratio with spacer thickness accompanied by a corresponding decrease of the F↓-conductance. This behaviour is probably related to the effective potential barrier in the d↓-channel due to the large difference between the Cu- and Co ↓ bands at the Fermi energy. For a narrower spacer, such a barrier allows for a larger transmission of electrons (see also Ref. [12]). The oscillations of the GMC ratio, namely a period of about 5 monolayers (ML) with a small admixture of the short-period oscillations of about 2.5 ML, are very likely due to the multiple scattering of the ↓-spin electrons at the system interfaces. The oscillation amplitude is approximately inversely proportional to the spacer thickness (see also Ref. [10]). However, the AF↓ conductances exhibit only strongly damped long-period oscillations with a period of about 5 ML.

The effect of the inserted Fe (Ni) monolayers at the interfaces (Fig. 2) is to increase the GMC ratio, in particular for the case of Fe. The origin of this increase is obvious from the plot of the partial conductances (Fig. 2b). The F↑ conductances for an ideal trilayer and for the trilayer with inserted Fe monolayers are almost the same because of the similarity of the Co↑- and the Fe↑ bands (both with a good matching to the spacer Cu bands), while the F↓ conductances of the trilayer with inserted Fe monolayers are reduced due to an additional potential barrier in the d↓-channel (the exchange splitting of Fe is larger as of Co). Together with the fact that the AF conductances for the trilayer with inserted Fe monolayers are reduced by approximately the same amount as the F↓ conductances, this gives rise to an increase in the GMC ratio in this case.

3.2. Diffusive transport

Disorder in a $Cu_{84}Ni_{16}$ spacer (Fig. 3) results in a strong suppression of the GMC ratio as compared to the ideal Co/Cu/Co trilayer. This can again be seen from the partial conductances (Fig. 3b). The decisive role played by F↑-spin electrons is obvious: despite the fact that the disorder is not very strong at the Fermi energy for this concentration [16], it reduces the originally high F↑ conductances much more than the F↓- and AF conductances. For the F↓- and AF conductances, the additional potential scatterings due to Ni impurities are thus relatively less relevant since they already undergo strong intrinsic scatterings at interfaces. The net result is a strong suppression of the GMC ratio.

In principle, for $n \to N_{\parallel}$, the supercell calculations are exact. We compared our results with CPA-type transport calculations neglecting vertex corrections. These results yielded conductances that were too small, indicating perhaps the necessity of including vertex corrections in the case of CPP transport.

Acknowledgements

Financial support for this work was provided by the Grant Agency of the Czech Republic (Project No. 202/97/0598), the Grant Agency of the Academy of Sciences of the Czech Republic (Project A1010829), the Center for Computational Materials Science in Vienna (GZ 45.442 and GZ 45.420), the Austrian Science Foundation (FWF P11626-PHY), the MŠMT of the Czech Republic (COST P3.70), the Austrian BMWV and the MŠMT of the Czech Republic (AKTION WTZ I.23), and the TMR Network 'Interface Magnetism' of the European Commission (Contract No. EMRX-CT96-0089).

References

[1] P.M. Levy, Solid State Phys. 47 (1994) 367.
[2] M.M. Baibich, J.M. Broto, A. Fert, F.N. Nguyen Van

Dau, F. Petroff, P. Etienne, G. Creuzet, A. Friedrich, J. Chazelas, Phys. Rev. Lett. 61 (1988) 2472.
[3] W.P. Pratt Jr., S.-F. Lee, J.M. Slaughter, R. Loloee, P.A. Schroeder, J. Bass, Phys. Rev. Lett. 66 (1991) 3060.
[4] K.M. Schepp, P.J. Kelly, G.E.W. Bauer, Phys. Rev. B 57 (1998) 8907.
[5] P. Zahn, I. Mertig, M. Richter, H. Eschrig, Phys. Rev. Lett. 75 (1995) 3216.
[6] W.H. Butler, X.-G. Zhang, D.M.C. Nicholson, J.M. MacLaren, Phys. Rev. B 52 (1995) 13 399.
[7] P. Weinberger, P.M. Levy, J. Banhart, L. Szunyogh, B. Újfalussy, J. Phys. Condens. Matter 8 (1996) 7677.
[8] C. Blaas, P. Weinberger, L. Szunyogh, P.M. Levy, C.B. Sommers, J. Phys. Condens. Matter 60 (1999) 492.
[9] J.A. Stovneng, P. Lipavský, Phys. Rev. B 49 (1994) 16 494.
[10] J. Mathon, Phys. Rev. B 56 (1997) 11 810.
[11] J. Cerdá, M.A. Van Hove, P. Sautet, M. Salmeron, Phys. Rev. B 56 (1997) 15 885.
[12] S. Sanvito, C.J. Lambert, J.H. Jefferson, A.M. Bratkovsky, Phys. Rev. B 59 (1999) 11 936.
[13] O.K. Andersen, O. Jepsen, Phys. Rev. Lett. 53 (1984) 2571.
[14] P. Bruno, H. Itoh, J. Innoue, S. Nonoyama, J. Magn. Magn. Mater. 198–199 (1999) 46.
[15] I. Turek, V. Drchal, J. Kudrnovský, M. Šob, P. Weinberger, Electronic Structure of Disordered Alloys, Surfaces and Interfaces, Kluwer, Boston, MA, 1997.
[16] B.L. Gyorffy, G.M. Stocks, in: Electrons in Disordered Metals and at Metallic Surfaces, P. Phariseau, B.L. Gyorffy, L. Scheire (Eds.), NATO ASI Series, Plenum Press, New York, 1979.